OLIVEIRA A., PEREIRA A.S., LEMOS P., GUERRA J.P., SILVA V., FARIA P. (2021), Effect of innovative bioproducts on air lime mortars. Journal of Building Engineering, 101985. https://doi.org/10.1016/j.jobe.2020.101985

EFFECT OF INNOVATIVE BIOPRODUCTS ON AIR LIME MORTARS

Alexandre Oliveira, CERIS, Departamento de Engenharia Civil, Faculdade de Ciências e Tecnologia, Universidade NOVA de Lisboa, an.oliveira@campus.fct.unl.pt

Alice S. Pereira, UCIBIO-REQUIMTE, Departamento de Química, Faculdade de Ciências e Tecnologia, Universidade NOVA de Lisboa, masp@fct.unl.pt

Paulo C. Lemos, LAQV-REQUIMTE, Departamento de Química, Faculdade de Ciências e Tecnologia, Universidade NOVA de Lisboa, paulo.lemos@fct.unl.pt

João P. Guerra, UCIBIO-REQUIMTE, Departamento de Química, Faculdade de Ciências e Tecnologia, Universidade NOVA de Lisboa, jp.guerra@campus.fct.unl.pt

Vitor Silva, Departamento de Engenharia Civil, Faculdade de Ciências e Tecnologia, Universidade NOVA de Lisboa, vmd.silva@fct.unl.pt

Paulina Faria, CERIS, Departamento de Engenharia Civil, Faculdade de Ciências e Tecnologia, Universidade NOVA de Lisboa, paulina.faria@fct.unl.pt (corresponding author)

Abstract

In this work, air lime mortars were bioformulated with two innovative bioproducts, one resulting from iron supplemented *Escherichia coli* cultures and a second one exploiting mixed multiple cultures grown with crude glycerol as substrate. The bioproducts were lyophilized and, for the mortar formulation, suspended in water and used as mixing liquid. Workability of mortars was evaluated by the flow table consistency and 90-days-old samples were tested for different properties, such as thermal conductivity, bulk density, porosimetry, water absorption, drying, surface hardness and compressive strength. With water content to ensure workability, bioformulated mortars presented higher thermal insulation and reduced water absorption when compared with a non-bioformulated control mortar. However, the presence of bioproducts decreased the compressive strength of the air lime mortar. Contact with water, simulating weathering, diminished that decrease. The strategy utilized in the present work meet some of the goals of a circular economy approach

maximizing natural resources by the use of wastes to produce the bioproducts and increasing lime mortars durability.

Keywords: Air-lime mortars, Bioformulation, Crude-glycerol-based mixed microbial cultures bioproduct, Durability, *Escherichia coli*-based bioproduct, Sustainability.

1. Introduction

Air lime mortars were vastly used in the past as masonry bedding mortars, for joint repointing, plastering and rendering (Veiga 2017). Air lime mortars suffer degradation such as erosion, cracks and detachments, often associated with climate conditions changes (temperature, relative humidity (RH), wind and rain). Veiga et al. (2010) stated that improper conservation and repair techniques, as well as lack of maintenance, can cause major deterioration. The decision for their partial or total replacement may result in widespread deterioration.

Due to their compatibility with original building materials, air lime mortars should be widely used in the conservation and repair of old constructions (Liu et al. 2018, Veiga 2017, Fang et al. 2015, Silva et al. 2015 and Botas et al. 2015). Although subjective and complex, compatibility occurs when mortars with similar composition attain the same chemical reactivity and physical characteristics (Hansen et al. 2003). In order to ensure compatibility, it is essential to determine the characteristics of the existing substrate, so that conservation replacement mortars can be developed with characteristics similar to those presented nowadays by the old ones (Rossi-Doria 1986;Van Hees et al. 2004; Damas et al. 2018, Faria et al. 2008). To comply with the principle of compatibility, replacement mortars must also meet aesthetic and functional requirements, while preserving the durability and integrity of historic buildings (Veiga et al. 2010).

Air lime mortars may have several limitations for application due to their intrinsic characteristics, such as high drying shrinkage, relatively low mechanical strength, high water absorption and porosity (Fang et al. 2015 and Liu et al. 2016). Its high drying shrinkage can be controlled by a re-compaction some hours after application, that is fundamental for renders and plasters, closing the drying cracks, decreasing porosity and increasing strength. However, that is difficult to be performed in laboratory common samples (Faria et al. 2008). On the other hand, they can also present

advantageous characteristics, such as high deformability, water vapor permeability and drying capacity. Some of these properties can be enhanced by biotechnology.

Biotechnology is based on the biological actions of cells or enzymes often involving precipitation of chemical compounds due to the bacterial culture's metabolism. The term bioformulation refers to the formulation and production of new construction composites, as mortars, using biological systems, bacterial cultures or enzyme that produce bioproducts. Bioformulation is not new, as vernacular bioformulated mortars were produced with organic products, from vegetable or animal origin, such as animal fat and vegetable oils (Nunes and Slížková 2014). Bioformulation may have a profound effect in the final composites since bioproducts included in the manufacture of those construction products strongly contribute to define their characteristics. These effects may be reflected in the consolidation of the construction products, by reducing erosion or contributing to waterproofing, thus reducing the absorption of water and increasing durability. Currently, bioformulation techniques to preserve historic constructions are a growing trend. This innovative methodology has recently been applied to different materials such as soil (Nakamatsu et al. 2017, Stabnikov and Ivanov 2016, Naeimi et al. 2016, Ivanov et al. 2014, Omoregie et al. 2017, Keykha et al. 2017), concrete (Zhang et al. 2017, Joshi et al. 2018, Vashisht et al. 2018, Seifan et al. 2018, Wang et al. 2018), cement mortar (Lors et al. 2017, Joshi et al. 2018, Luo et al. 2018, Son et al. 2018, Schwantes-Cezario et al. 2020) and earth mortar (Aguilar et al. 2016, Dove et al. 2016). Bioformulation of earth materials can also be found in nature as in termite mounds (Gandia et al. 2019).

Considering air lime mortar bioformulations, some studies have been conducted aiming to reproduce ancient practices, with the addition of oils, plant and animal products. Table 1 summarizes the effects of some of these studies performed in the last decade with calcitic air lime mortar bioformulations, both slaked as a powder or a putty (Faria and Martins, 2013).

Table 1. Effect of some bioproducts on air lime mortars in comparison to reference mortars (red color indicates a disadvantages outcome, green color indicates an advantageous result)

Bioproduct	Use of the bioproduct	Air lime type	Lime: sand (vol.)	Sample dimensions (cm x cm x cm)	Cure time (days)	Bulk density (%)	Porosity (%)	Capillarity coefficient (%)	Total water absorption by capillarity (%)	Compressive strength (%)	Reference
Pig blood	Mixing water replacement	Powder	-	5 x 5 x 1	28			-98			Fang et al. (2015)
Nopal powder	Added to mixing water		1:3	5 x 5 x 5	28		-14 *			46	Ventolà et al. (2011)
Nopal mucilage							-24 *			6	
Animal glue							-38 *			92	
Casein							-17 *			68	
Olive oil							-52 *			53	
Areca nut (5%)	Added to mixing water		1:3	5 x 5 x 5	90	2			-46	22	Gour et al. (2018)
Linseed oil	Added to the dry material		1:3	4 x 4 x 16	180		16	-98	-77	-17	Nunes and Slížková (2014)
Carboxymethyl cellulose	Added to the dry material		1:2	5 x 5 x 5	28		10			~ 91	Liu et al. (2016)
Hydroxypropyl methylcellulose	Added to the dry material		1:1	4 x 4 x 16	91	-5.4	11	16		-8	Izaguirre et al. (2011)
Guar gum derivative						-5.4	5	-17		-15	
Cactus mucilage	Mixing water replacement	Putty	-	5 x 5 x 5	45		-0.4	-5	-14	~ 14	Molina et al. (2014)
Carbonic anhydrase enzyme	Added to the material		1:3	4 x 4 x 16	90					~ 14	Cizer et al. (2017)
Used cooking oil (UCO)	Added to the material		1:3	4 x 4 x 4 4 x 4 x 2 4 x 4 x 1	240		18	-96	~ -75	~ -47	Pahlavan et al. (2018)
Albumen							32	-5.5	~ =	~ -38	
UCO + albumen							23	-96	~ -70	~ -76	

* Comparison of the pore volume (cm^3/g) of the bioformulated mortar in relation to the control mortar

Some studies did not define the mortar proportions of lime:sand (in volume or weight), but for the majority of mortars the volumetric proportions air lime:sand were 1:3. Some of the mortars were tested after only 28 days of age what can be brief to ensure advanced carbonation of the air lime matrix. Porosity (or bulk density) and compressive strength seem to be the most tested properties of the air lime bioformulated mortars. While the majority of bioproducts applied decreased the mortars capillarity coefficient, its influence on porosity and compressive strength is varied. However, it seems common an increase on porosity (or decrease in density), associated with a decrease on compressive strength.

Very few studies of bioformulated lime mortars with bioproducts based on bacterial cultures have been reported. A previous study investigated the efficacy of surface treatments of an earth-based plastering mortar with bioproducts produced by *Escherichia (E.) coli* cultures supplemented with iron (EC+Fe) (Parracha et al. 2019). These bioproducts significantly increased the water resistance

capacity of the mortar, acting as compatible light waterproofing agents. These studies were extended to other construction materials: earth blocks, brick, limestone, air lime and cement mortars (Garcia-González et al. 2020). In this case the effect of an innovative sustainable bioproduct prepared from mixed microbial cultures (MMC) grown with crude glycerol from an industrial residue (biodiesel production) was also explored. The effect of the biotreatments reported by Garcia-González et al. (2020) was an increase in the time for water absorption by the different materials. Therefore, the efficacy of both types of bioproducts (EC+Fe and MMC) as light waterproofing external treatment agents was demonstrated. Bioformulations using the above mentioned bioproducts may have great potential, namely for architectural conservation mortars.

In the present work, the effect of EC+Fe and MMC bioproducts in air lime mortars bioformulations was assessed from fresh to hardened properties, with the aim of reducing water absorption. Different physical and mechanical properties of bioformulated air lime mortars were evaluated and compared with a non-bioformulated control: fresh state behavior through the flow table consistency and hardened state properties, such as thermal conductivity, bulk density, porosimetry, surface hardness, compressive strength, water absorption and drying, after 90 days.

2. Materials and methods

2.1. Common materials and bioproducts

An industrial powder hydrated air lime EN 459-1 (2015) CL90-S from Lusical, Lhoist Group, was used as binder. The chemical composition of the same air lime was assessed elsewhere (Gameiro et al. 2014). The air lime presented a loose bulk density equal to 0.391 kg/dm³. A river sand, with a loose bulk density of 1.539 kg/dm³, was used as aggregate. Particle size distribution of sand was determined according to EN 1015-1/A1 (1998/2006) and is presented in Table 2.

Table 2. Particle size distribution of sand

Sieve number	3/8”	4	8	16	30	50	100	200
Mesh (mm)	9.50	4.75	2.36	1.19	0.600	0.300	0.150	0.075
Passing (%)	100.0	99.3	92.8	72.1	40.6	12.0	2.7	0.7

Two bioproducts were used for bioformulation of air lime mortars. Both bioproducts have been described elsewhere (Parracha et al. 2019 and Garcia-González et al. 2020) when used as protective surface coating. Briefly, the EC+Fe was prepared from *E. coli* cultures grown in the LB medium, a nutritionally rich medium (10 g of tryptone, 5 g of yeast extract and 10 g of NaCl, pH ~ 7.0) supplemented with iron. The MMC bioproduct was obtained from cultures cultivated with crude glycerol as substrate, resuspended in water for a defined fresh cell concentration, and the cells submitted to lysis. Both bioproducts suspensions were freeze dried to remove the aqueous phase and stored at room temperature in sealed Falcon tubes protected from the light. Before use, they were resuspended in tap water at a concentration of 2 g/dm^3. This strategy makes the storage and preparation of the bioproducts for use on site facilitated.

The color of both bioproducts suspensions, using the Adobe Photoshop software, and the viscosity of the MMC bioproduct were analyzed (Figure 1). The MMC bioproduct suspension presented a gold color (RGB 195, 170, 76 – Pantone 7562C - Figure 1, a) and EC+Fe bioproduct presented a khaki color (RGB 178, 172, 150 – Pantone 7535C – Figure 1, b). The viscosity growth curve as a function of the shear rate was performed with a rotational rheometer Bohlin Gemini HR^{nano} and in the same laboratory environmental conditions (temperature of 20 ± 2 °C and 62 ± 5% RH).

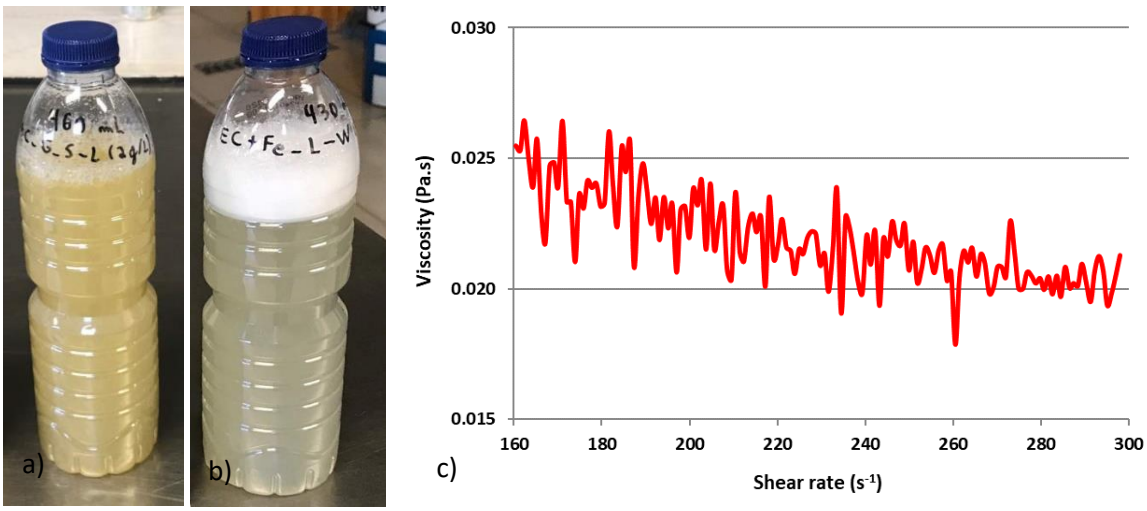

Figure 1. Color of the bioproducts MMC (a) and EC+Fe (b) and viscosity of the MMC bioproduct (c).

The apparent viscosity of the MMC bioproduct varied between 0.026 and 0.018 Pa.s for MMC bioproduct, as shown in Figure 1c. The MMC bioproduct was classified as a pseudoplastic fluid and considered appropriate for bioformulation, due to its low viscosity. Oliveira et al. (submitted) obtained similar results for the viscosity of the EC+Fe bioproduct, varying between 0.02 and 0.04 Pa.s using, however, a lower suspension concentration (0.7 g/dm^3). The bioproduct EC+Fe used in this work apparently had a slightly higher viscosity than the previous mentioned, due to its higher concentration (2.0 g/dm^3).

Figure 1 also shows that the EC+Fe bioproduct presents more foam in comparison to the MMC bioproduct, attributed to denaturation of biological molecules.

2.2. Production of mortars and curing

Three identical batches of mortars with an air lime:sand volumetric ratio of 1:3 were produced (six samples of each mortar). The same weight of dry components (powder hydrated air lime and sand) was used for all the mortars. From the loose bulk densities of each dry material, mortars were prepared with mass proportion of 1:11.8 (air lime:sand). The batch of non-bioformulated control mortar (C), was prepared with tap mixing water. In the bioformulated mortars, the mixing water was replaced either by the EC+Fe or by the MMC bioproducts liquid suspensions. The liquid content (tap water or bioproduct suspension) was decided to be the one that allowed an experienced technician to produce workable air lime mortars, that he was able to apply on-site as a render. Therefore, it was not decided to fix the mixing liquid content because that could lead to mortars not able to be applied. Thus, the liquid content was added to each mix and registered. The amount of water used for the Control mortar was 185 mL and the amount bioproduct suspension for the bioformulated mortars was 175 mL and 200 mL, respectively for EC+Fe and MMC. To validate its influence on mortars, fresh state consistency was assessed by flow table (EN 1015-3, 1999). It was not decided either to fix the consistency because the scientific community researching on air lime mortars is discussing the validity of this test, namely within RILEM TC 277 - LHS: Specifications for testing and evaluation of lime-based repair materials for historic Structures.

The solid mortar samples were produced by manually filling cylindrical PVC molds with a height of 2 cm and a diameter of 6.8 cm. Samples had a mold circular bottom surface and a less regular surface resulting from regularization with a trowel. Demolding took place 60 days after casting at a temperature of 22 ± 2 °C and RH of 65 ± 5 %, by cutting the PVC molds. Mortar samples were left to cure for extra 30 days, with the base elevated to facilitate carbonation by the bottom surface as well.

Characterization of mortar samples was performed in the fresh state (flow table consistency) and in the hardened state after 90 days (Figure 2).

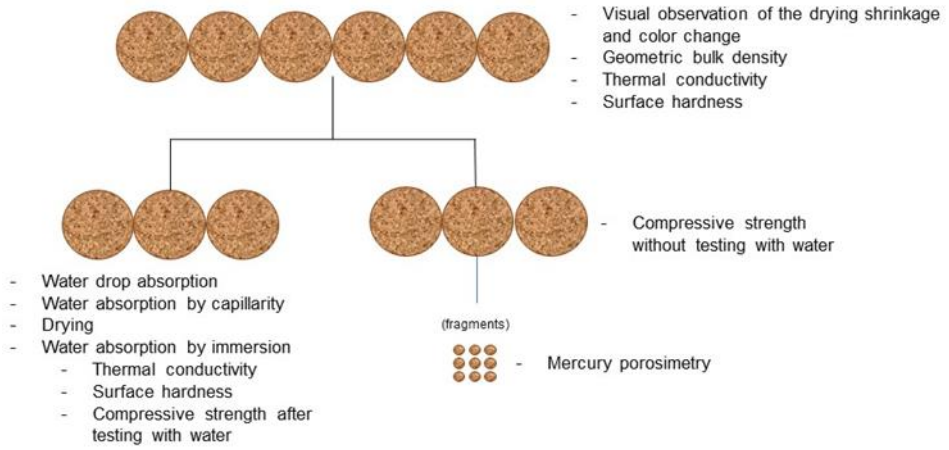

Figure 2. Schematic representation of testing campaign of mortar samples

2.3. Hardened state test procedures

Drying shrinkage and color change were assessed visually before demolding the samples. Thermal conductivity, surface hardness by durometer and compressive strength tests were performed after curing. The same tests were repeated after samples placed in contact with water and subsequent drying for simulating accelerated weathering conditions (Figure 2).

Capillarity, drying and immersion water absorption tests were performed under hygrothermal conditions of 21 ± 3 ° C temperature and 54 ± 6% RH.

Drying shrinkage, thermal conductivity, bulk density and porosimetry

Drying shrinkage was assessed visually by the difference of the samples to the molds, before being demolded. One of the most important requirements when using a product in conservation of building materials and works-of-art is aesthetics, which should not be significantly affected (Franzoni et al.

2014). Therefore, the top surface of all samples was visually observed before demolding with a Kodak® color scale. The odor of the samples was analyzed after curing.

Thermal conductivity of mortars was determined before and after the water immersion test, with an ISOMET 2104 Heat Transfer Analyzer equipment, with a 60 mm diameter contact probe API 210412 applied on the molded circular surface of samples (Figure 3). Samples were previously stabilized in a conditioned room at a temperature of 21 ± 3 °C and 54 ± 6 % RH and placed on top of an expanded insulation cork board (Figure 3). During the tests the samples were at a temperature of 23 °C and 57 ± 1 % RH (before water tests) and a temperature of 24 °C and 62 ± 1 % RH (after water tests).

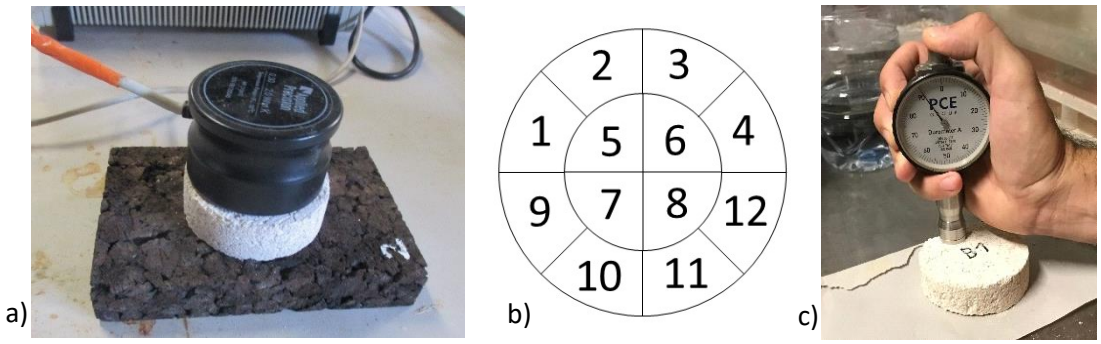

Figure 3. Thermal conductivity testing (a) and surface hardness measurement scheme (b) and testing a sample (c)

Bulk density was carried out based on EN 1015-10/A1 (1999/2006). The diameter and height of each sample were measured with a digital caliper with precision 0.01 mm and the mass was determined using a 0.001 g precision scale. The average bulk density (kg/dm³) was calculated from the ratio of mass (kg) to the volume of each mortar prism (dm³).

The porosimetric distribution of each mortar was determined by the mercury porosimetry intrusion (MIP) test with a Micromeritics AutoPore IV equipment. Samples were previously equilibrated at a temperature of 21 ± 3 °C and 54 ± 6 % RH. The test was performed with low pressure up to 172.4 kPa (25 psi) and the high pressure ranged between 206.8 kPa (30 psi) and 206.8 MPa (30,000 psi).

Water absorption (drop, capillarity, immersion) and drying

Water drop absorption was carried based on RILEM II 8b (1980), adapted by Parracha et al. (2019). This test consists on measuring the time for a drop of water to be absorbed by the top surface of a

sample. Therefore, one drop of water (0.1 mL) was applied to four separated areas of the circular sample using a micropipette, with a fixed distance of 1.5-2.0 cm between the micropipette tip and the tested surface. The time until each water drop was completely absorbed was video recorded. This test was carried out under hygrothermal conditions equal to the previous test. For this analysis Z-score statistical method was used as described by Oliveira et al. (submitted), to reduce data dispersion and to exclude data that deviated too far from the mean value. The incremental time (or delay time) relative to the control for each campaign/application method was also used as defined by Oliveira et al. (submitted).

Water absorption by capillarity was determined with the top surface of samples in contact with water, based on EN 15801 (2009), with unprotected lateral surfaces. Samples were equilibrated in a conditioned room in hygrothermal conditions, as mentioned before. Samples were initially weighted using a 0.001 g precision scale and placed on a thin plastic net, so that the bottom surfaces were in total contact with a 2 mm water film, inside a sealed box with saturated RH. Masses of samples were measured every minute during the first 5 minutes, and then at 7 and 10 minutes. Subsequently, the weight was assessed every 5 min between up to 45 minutes and after at every hour up to a total of 5 hours of testing. Samples were also weighed after 24 and 48 hours. Before each measure the excess of water at the bottom surface was removed by rapid contact with a damp tissue. The water height was maintained throughout the test.

The amount of water absorbed after each defined time of water contact was calculated. The capillarity curve allowed to calculate the average capillarity coefficient and asymptotic value for each mortar. Capillarity coefficient of the mortars was calculated by the slope of the straight segment defined by the initial part of the curve. The asymptotic value of the capillarity curves represents the total amount of water absorbed by each mortar.

Drying test was performed after the water absorption by capillarity test (with the samples still completely saturated with water). It was determined based on EN 16322 (2013), with the top surface of samples, now upwards, and the other circular surface in contact with a waterproof surface, blocking drying by that surface. As reported in the capillarity water absorption test, the lateral

surfaces of samples were not waterproofed. Thus, the lateral area of the samples was considered for drying, together with the top surface. The first mass reading (t = 0) corresponds to the last weighing of the sample in the capillarity test (maximum mass). In the first hour of the test, samples were weighed every 10 min. After the first hour, the measurements occurred every hour until the next 7 h. Subsequent measurements were then performed twice daily with a minimal interval of 8 h between the two successive measurements over the next 2 days. Finally, subsequent measurements were performed once a day for the next 2 days, ending the test upon reaching 1 % mass difference between two consecutives weighing's. The residual amount of water present in the sample per unit area is determined for each weighing.

The drying curves of each sample was determined and the average drying rates, in the 1st and 2nd drying phases, were calculated for each mortar. The drying rate of the samples in the 1st drying phase was found by the slope of the straight segment defined by the initial masses of the drying curve per time, while the one in the 2nd drying phase was obtained by the slope of the straight segment at an intermediate period of the drying curve per square root of time.

The drying index for each sample was also calculated by the drying curve using the integral defined in EN 16322 (2013) after a defined period of time. In the present case, it was determined after 48 h. Water absorption by immersion test of samples was carried out in accordance to EN 772-21 (2011), using a desiccator since the samples could not be dried in an oven, due to the existence of organic components. They were stabilized in hygrothermal conditions equal to the previous tests. Samples were weighted with a scale with an accuracy of 0.001 g and placed in a desiccator where they were immersed in water. After 48 h, samples were removed from the water and, with a wet towel, the superficial excess of water was removed and immediately weighted. After this process, the percentual water absorption was determined.

Surface hardness and compressive strength

Surface hardness was determined based on ASTM D2240 (2000), with a PCE durometer Shore A (PCE Instruments). The scale of the durometer ranges from 0 to 100. Surface hardness was evaluated before and after the tests with water at 12 different points (Figure 3, b) along the molded surface of

each sample (Figure 3, c).

Compressive strength of mortar samples was determined according to EN 1015-11 (1999) using a Zwick Rowell Z050 equipment with a 50 kN load cell and test speed of 0.7 mm/min. The compression area was 40 mm x 40 mm and was guaranteed by two very hard basalt pieces, aligned, one placed above and another below each mortar sample. The test was performed both for samples that did and did not went through water tests (Figure 2).

3. Results and discussion

3.1. Fresh state characterization

The control mortar presented a mixing liquid/binder ratio of 2.4 and a consistency of 168 mm. The EC+Fe bioformulated mortar had lower flow table consistency (162 mm) and lower mixing liquid/binder ratio (2.2) than the control mortar but was more workable and homogeneous than the control mortar. The MMC bioformulated mortar presented the highest flow table consistency (182 mm) but also higher mixing liquid/binder ratio (2.5).

The MMC mortar seemed to need a higher liquid content to be mixed with adequate workability, which can explain its higher flow, and later exuded more and was less homogeneous. Also, Nunes and Slížková (2014) to maintain the same consistency in mortars bioformulated with linseed oil had to add a slightly larger amount of water. Their explanation was that the particles of the binder were covered with oil preventing water absorption. Although that should not be the case in the present work, the presence of more hydrophobic molecules produced by the cell, as lipids or other organic metabolites such as polymers from the glycerol metabolism, could explain the observed behaviour. Therefore, in comparison to the control mortars, it was more difficult to produce the MMC mortar and easier to achieve a very workable EC+Fe mortar.

3.2. Hardened state characterization

3.2.1. Drying shrinkage, visual observation of color change and odor detection

At the time of demolding there was no significative visual shrinkage of any of the mortars inside the molds. No change in color could be visually observed on the surfaces of the bioformulated air lime

mortar samples in comparison to the control. Similarly, Pahlavan et al. (2018), evaluating the performance of air lime mortars formulated with two organic waste additives - used cooking oil and albumen - did not observe any color changes with the naked eye. No differences in odor could be detected after the curing of the samples.

3.2.2. Bulk density and porosimetry

Average and standard deviation of bulk density of the mortars are listed in Table 3.

Table 3. Average and standard deviation of the geometric bulk density

Bulk density (kg/dm^3)		
Mortar	Average	Sd
C	1.83	0.02
EC+Fe	1.76	0.04
MMC	1.75	0.04

The average bulk density of bioformulated mortars was slightly lower (approximately 4 %) compared to the control, indicating a more porous microstructure, probably due to a poor packing caused by the presence of polydisperse biological molecules from the bioproducts. A similar effect was observed by Izaguirre et al. (2011) for 3-month-old air lime-based mortars bioformulated with two different commercial water retention additives, a hydroxypropyl methylcellulose and a guar gum derivative, that found a decrease of 5.4 % of the density of both mortars relative to control (Table 1). In contrast, Gour et al. (2018) obtained an increase of up to 2 % in bulk density, when studying air lime mortars using areca nut natural polymer (Table 1).

Figure 4 shows bimodal pore size distribution curves of the porous microstructure assessed by MIP.

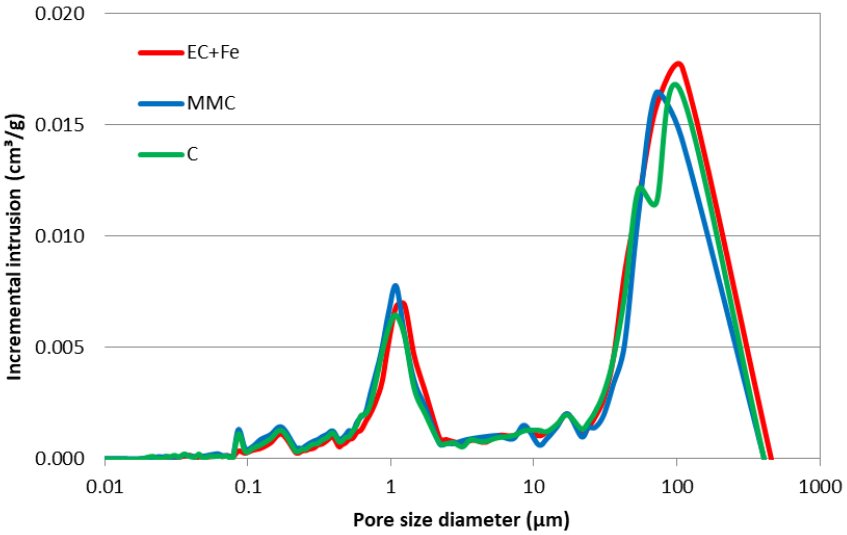

Figure 4. Pore size distribution of bioformulated and control mortars

The more frequent pore size diameter of all the mortars, and also of the control mortar, is high. This can possibly be assigned to shrinkage cracks (Nunes and Slížková, 2014). Such as in the present study, Nunes and Slížková (2014) also found a bimodal porosimetric distribution for CL90-S air lime mortars and more frequent pore size diameter of 86 µm. When they added linseed oil to the mortar formulation, the diameter increased to around 95 µm. Silva et al. (2020) for CL80-S air lime mortars obtained a diameter of around 90 µm.

There are two distinct pores diameter main ranges: 0.8 - 1.6 µm and 45 - 250 µm. In the first range those were slightly more abundant for bioformulated mortars in relation to the control mortar, while in the second range EC+Fe mortar had the highest numbers. For the smaller pores all mortars have a median diameter around 1.1 µm. It was also observed that the control mortars presented two regions of pores in the high range, at 54 µm and 108 µm, while bioformulated mortars have just one each, 110 µm for the EC+Fe and 72 µm for the MMC. This fact may justify the result of the bulk density, since the control sample had greater bulk density in comparison to the bioformulated mortars.

These results were similar to those found by other researchers: Nunes and Slížková (2014), when studying the influence of linseed oil for 6-month-old air lime mortars, found a 16 % increase in porosity; Izaguirre et al. (2011), when analysing 3-month-old air lime mortars formulated with

hydroxypropyl methylcellulose and a guar gum derivative, found an increased porosity of 11 % and 5 %, respectively (Table 1). However, in the opposite direction, Ventolà et al. (2011) found a 14 % reduction in porosity, when analysing bioformulated 28-days-old air lime mortars with polysaccharides (nopal used as powder). Therefore, it seemed that the changes in density (and, expectedly, in porosity), depended on the type of bioproduct but those were not very significant.

3.2.4. Thermal conductivity

Thermal conductivity of mortars, before and after the water tests, is presented in Figure 5.

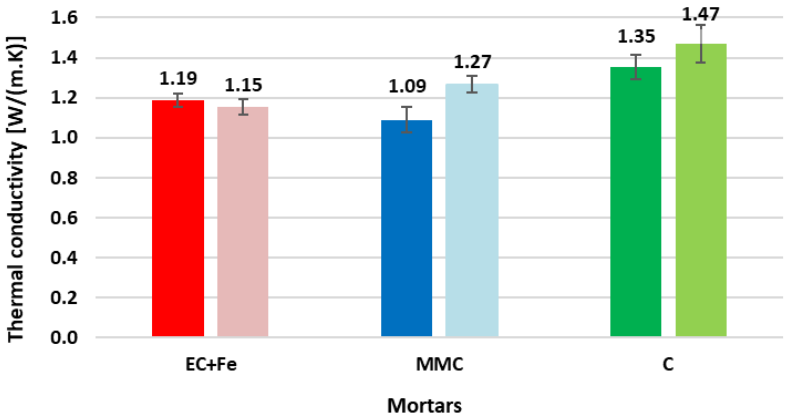

Figure 5. Average and standard deviation of thermal conductivity conducted before (to the left) and after (to the right) the water tests

Bioformulated mortars presented a thermal conductivity lower than the control, both before and after water testing, indicating that bioformulation improved thermal insulation over traditional mortars. The data was in agreement with the decrement of the bulk densities observed. Compared to the control, the decrease of the thermal conductivity of the EC+Fe mortar before and after the water tests were 12 % and 22 %, respectively and the reductions achieved by MMC mortar were 20 % and 14 %, respectively. After the water test, thermal conductivity of the MMC and control mortars increased (17 % and 9 %, respectively). This may result from the contact with water allowing an increase of porous structure filling, what is in agreement with self-healing capacity of lime mortars (Nardi et al., 2017). Tests with water did not significantly affect the thermal conductivity of EC+Fe mortar, being the obtained value 3 % lower than the one before testing that can be considered within the experimental error.

3.2.5. Water absorption (drop, capillarity, immersion) and drying

The results of the application of different methods to assess the water absorption capacity of bioformulated mortars are summarized on Table 4.

Table 4. Water absorption and drying properties (average and standard deviation).

Tests	Mortars		
	EC+Fe	MMC	C
Drop:			
Time to absorb a drop of water [s]	158 ± 28	176 ± 45	22 ± 14
Capillarity:			
Capillarity coefficient [kg/(m².s$^{1/2}$)]	0.201 ± 0.017	0.287 ± 0.027	0.347 ± 0.006
Total water absorption by capillarity [kg/m²]	3.963 ± 0.024	4.236 ± 0.021	4.251 ± 0.033
Immersion:			
Water absorption by immersion [%]	11.1 ± 0.5	11.9 ± 0.1	11.9 ± 0.3
Drying:			
Drying rate – 1st phase [kg/(m².h)]	0.115 ± 0.005	0.102 ± 0.007	0.118 ± 0.011
Drying rate – 2nd phase [kg/(m².h$^{1/2}$)]	0.480 ± 0.016	0.486 ± 0.003	0.508 ± 0.006
Drying index at 48h	0.138 ± 0.001	0.141 ± 0.001	0.141 ± 0.001

The water drop test results showed that bioformulated mortars significantly slow down water absorption compared to the control mortar. The difference when a drop contacted the control and bioformulated samples were visible. The delay time of EC+Fe and MMC mortars was approximately 610 % and 700 %, respectively, relative to the control. Parracha et al. (2019) used this non-standardized test to evaluate the effect of EC+Fe bioproduct on the water absorption of surface treated earth plasters. The researchers found a significant improvement of the resistance to water ingress capacity compared to the control samples.

Average capillarity water absorption curves for each mortar (control, EC+Fe and MMC) are shown in Figure 6.

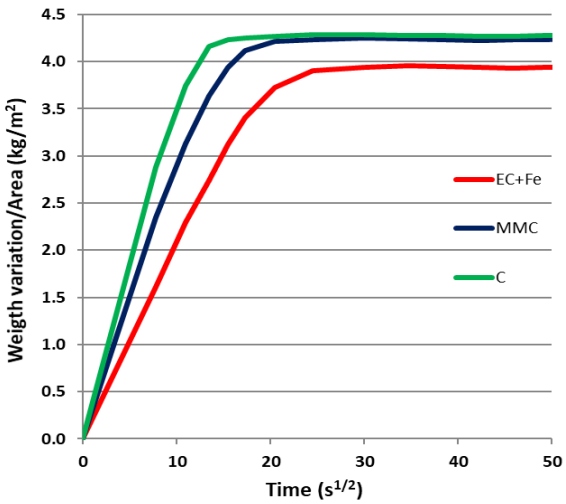

Figure 6. Average curves of water absorption by capillarity of each mortar

The data of Figure 6 and Table 4 showed that both bioformulated mortars presented a lower capillarity coefficient in comparison to the control. These results may be explained by the hydrophobic effect occurred by the presence of organic compounds (Schaumann et al., 2007). The EC+Fe bioproduct had a very positive effect, since the bioformulated EC+Fe mortar absorbed less water, and slower than the MMC mortar and the control. Mixing with the EC+Fe bioproduct had a great impact on the mortars, decreasing the capillarity coefficient by 42 % compared to the control, while the reduction in total water absorption reached 7 % (Table 4). A similar reduction was also reported by Gour et al. (2018), that achieved a 46 % decrease on total water absorption by capillarity on air lime mortars bioformulated with areca nut (Table 1), explained by the hydrophobic nature of the polymer used. Although more modest, MMC mortar showed a 17 % reduction in the capillarity coefficient while no significative changes in the total water absorbed by capillarity relative to the control was detected.

Molina et al. (2014), when studying air lime mortar with cactus mucilage, obtained a 5 % reduction in the capillarity coefficient (Table 1). The researchers explained the data by the formation of whewellite and weddellite crystals that filled the pores of the mortar. Similarly, Pahlavan et al. (2018) obtained a 5.5 % reduction in the capillarity coefficient investigating air lime mortars prepared with albumen. Therefore, the reduction of capillarity coefficient obtained by both tested bioproducts, and particular the EC+Fe, seems very promising in comparison to other bioproducts

that have been studied for air lime mortars.

When analyzing the results of the water absorption by immersion (Table 4), it can be concluded that the water absorption capacity of the EC+Fe mortar decreased by 6.7 %, while both MMC and control mortars presented identical values. This was in agreement with results of total waster absorbed.

The drying curves, with segments that allowed determination of the first and second drying phases rates (Table 4), are presented in Figure 7.

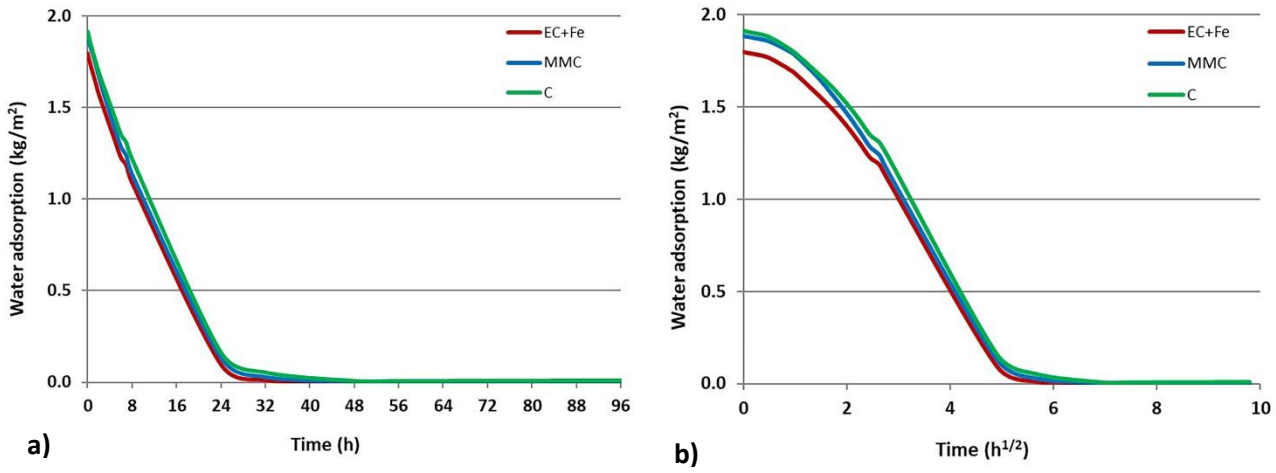

Figure 7. Average drying curves, to calculate the first (a) and the second (b) drying rates of each mortar

The drying curves of bioformulated mortars are very similar to the control mortar. Therefore, the effect of bioproducts on drying was acceptable, not jeopardizing the compatibility of the bioformulated mortars. Analysis of curves and drying rates in the first drying phase, allowed to conclude that the MMC mortar had a smaller initial drying capacity (14 % reduction), while EC+Fe and control mortars presented identical capacities. In the second drying phase, decrements of 6 % and 4 % for EC+FE and with MMC bioformulated mortars were observed, relative to the control mortar. The results of the drying index after 48 h of test showed that both bioformulated mortars had a total drying capacity similar to the control. As so the bioproducts do not significantly interfere with drying, in each phase and globally.

The differences observed for EC+Fe and MMC mortars seemed to indicate that the first ensured a more effective capacity towards several water tests, with greater reductions in capillarity absorption coefficient and total amount of water absorbed, as well as a good increase on water drop adsorption

time. However, the changes do not seem to affect compatibility as drying capacity was not significantly reduced.

3.2.6. Surface hardness

Surface hardness results, before and after water tests, are shown in Figure 8.

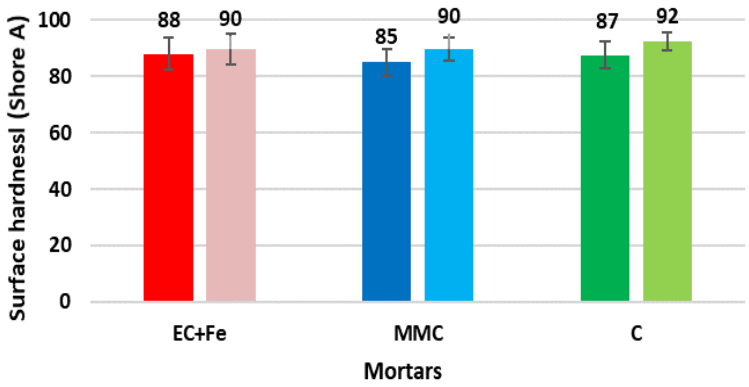

Figure 8. Average and standard deviation of the surface hardness of mortars, before (to the left) and after (to the right) water tests

Surface hardness results of bioformulated mortars were, within the experimental error, similar to the control, before and after the water tests. However, all values tended to increase after water tests, may be due to a self-healing effect of mortars (Nardi et al., 2017). These results are similar to those found by Parracha et al. (2019), when studying the efficacy of iron-supplemented *E. coli* cultures as a surface bioproduct for earth-based plastering mortars. In the present work, the bioproducts also allowed to ensure compatibility of bioformulated air lime mortars with conventional ones.

3.2.7. Compressive strength

Compressive strength of mortars was determined before and after water tests (Figure 9).

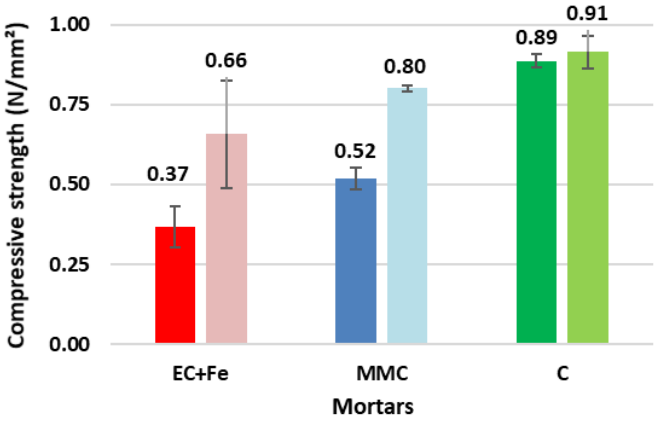

Figure 9. Average and standard deviation of the compressive strength of mortars, before (to the left) and after (to the right) water tests

The presence of both bioproducts reduced the compressive strength of air lime mortars. This fact is in agreement with the results of MIP, because the control mortar has a smaller total volume of pores in the two distinct pore sizes ranges (Figure 4), and higher bulk density that may have favored their higher compressive strength. The decrease was more significant for the EC+Fe mortar before water testing, with a reduction of 58 % for the EC+FE mortar, in comparison to 42 % for the MMC mortar, relative to the control. Therefore, the effect of a probable slight water repellency of the bioformulated mortars seemed to be stronger for carbonation, in comparison to its lower density (and higher porosity). However, for both bioformulated mortars, the contact samples had with water in some tests, simulating accelerated weathering, produced a significative increase of compressive strength, while the increase was minimal for the control mortar. After the tests with water contact, the reduction of compressive strength decreased in both cases by ~30 %, corresponding only to 28 % and 12 % reduction for EC+Fe and MMC mortars, relative to the control. These results may probably be explained by the progression of carbonation (Delgado Rodrigues 2020), that was retarded in comparison to the control, just as it happened with Nunes and Slížková (2014) and Nunes et al. (2020), when studying bioformulated air lime mortars with linseed oil (Table 1). Comparing with previous studies in the literature (Lanas and Alvarez, 2003; Lawrence et al., 2006; Garijo et al., 2020), it is sure that the control mortar of the small cylindrical samples, tested after 90 days curing in conditions of 22 ± 2 °C temperature and 65 ± 5 % RH, were considered carbonated. Therefore, the carbonation test of mortars was not performed. However, this test is foreseen for future studies, as it seems possible that the bioproducts can have an effect on the carbonation process.

An additional explanation could be a self-healing effect that may happen in all the mortars, that is usual to air lime composites (Nardi et al., 2017), although commonly needing more time. Nevertheless, the compressive strength of the control mortar did not change significantly after water testing, what shows that self-healing was unlikely. Within the experimental error, all mortars were in the range of rendering/plastering mortars defined by Veiga et al. (2010) for historic masonry and only

EC+Fe mortars tested before the water test did not achieved the minimum value defined by EN 998-1 (CEN, 2016) of 0.4 N/mm^2, to be classified as general purpose rendering and plastering mortar.

Similar reductions in compressive strength of bioformulated air lime mortars were reported in the literature. Nunes and Slížková (2014) observed a 17 % reduction in compressive strength of linseed oil for 6-month-old air lime mortars. Pahlavan et al. (2018) found a reduction of 47% and 38% for 8-month-old air lime mortars with used cooking oil and albumen, respectively. Izaguirre et al. (2011) registered a reduction of about 8 % and 15 % for 3-month-old air lime mortars with hydroxypropyl methylcellulose and guar gum, respectively. Contrarily to the present and previously mentioned studies, some researchers achieved an increase in compressive strength. Ventolà et al. (2011) reported a 6 % increase analysing bioformulated 28-days-old air lime mortars with polysaccharides (nopal mucilage) and Gour et al. (2018) achieved an increase of 22% using 3-month-old air lime mortars with areca nut natural polymer (Table 1). In fact, distinct results may be associated with the wide diversity of bioproducts used to prepare air lime mortars in different experimental conditions (not all defined in the respective articles), affecting the physical and mechanical properties of the final material.

4. Conclusion

In this study, air lime mortars bioformulated with two innovative bioproducts, one produced by *Escherichia coli* cultures grown in rich medium supplemented with iron and a second by mixed microbial cultures produced with crude glycerol, were analysed. The results showed a very good workability of the mortar bioformulated with the *E. coli* bioproduct and, after 90 days curing, a slight reduction in bulk density for both bioformulated mortars. Yet, incorporation of bioproducts in the formulation did not significantly alter the microstructure of mortars, although it could justify the lower density and thermal conductivity.

Regarding the increase of time to absorb a drop of water, a significant improvement in both bioformulated mortars was observed, indicating that these mortars may provide enhanced protection against direct contact of rainwater in comparison to conventional air lime mortars, what can be of

particularly importance for unpainted masonry joints and renders.

In general, the EC+Fe mortar presented lower water absorption than the MMC mortar and the control mortar. In addition, the bioproducts did not reduced the air lime mortar drying capacity. However, the MMC mortar had higher compressive strength than the EC+Fe mortar, both bioformulated mortars being significantly less resistant than the control mortar. The decrease on bioformulated mortars compressive strength clearly reduced on mortars tested after contact with water, simulating natural aging to rising damp and rain. These results suggested that bioproducts may induce a delay in mortars carbonation and/or the need of a more humid curing. Importantly, no significative shrinkage, change in color or brightness was visually observed on the surfaces of bioformulated mortars when compared to the control. No odor could be detected.

The results confirm that the partial or total replacement of old air lime mortars by these innovative bioformulated air lime mortars will reduce thermal conductivity and water absorption, without substantially interfering with mortar properties relative to drying, ensuring compatibility with historic masonries. However, the effect of the bioproducts on carbonation and compressive strength, including curing conditions, should be further studied.

The utilization of bioproducts in the formulation of different types of materials is a growing trend. The two proposed here find different approaches for its production. The EC+Fe depends on the growth of a pure microbial culture while the MMC utilizes a diverse microbial composition. Those bioproducts present some costs of production, higher in the case of *E. coli* bioproducts due to the need of sterility in the process. The utilization of a waste/by-product as substrate in the case of MMC - crude glycerol resulting from the production of biodiesel - also contributes to a lower cost of production and to the sustainability of the all process. The strategy utilized in the present work meet some of the goals of a circular economy approach maximizing natural resources, by reusing waste/by-product stream of other processes into new ones, as well as more efficiently managing the introductions of new materials in the construction conservation process. In the case of *E. coli* even though the process for growing biomass would be more expensive, their efficiency was somehow better in the bioformulation process. The iron utilized for the EC process could be provided by an

industrial waste, contributing also for the sustainability and the circular economy.

Acknowledgements

The authors acknowledge Prof. Luís Baltazar, for the support on rheological characterization of the bioproducts, and to the Portuguese Foundation for Science and Technology (FCT) for the financial support within research project PTDC/EPH-PAT/4684/2014: DB-Heritage - Database of building materials with historical and heritage interest. This work was supported by the Civil Engineering Research and Innovation for Sustainability Unit-CERIS, Applied Molecular Biosciences Unit-UCIBIO-REQUIMTE and Associate Laboratory for Green Chemistry-LAQV-REQUIMTE, which are financed by national funds from FCT (UIDB/04625/2020, UIDB/04378/2020 and UID/QUI/50006/2020, respectively) and co-financed by the ERDF under the PT2020 Partnership. João P. Guerra is supported by the Radiation Biology and Biophysics Doctoral Training Programme (RaBBiT- PD/00193/2012 and CEFETIC- UIDB/00068/2020) and a PhD fellowship (PD/BD/135476/2017) from FCT. Paulo C. Lemos acknowledge the support by FCT for contract IF/01054/2014/CP1224/CT0005. Finally, to the Court of Accounts of the State of Ceará - TCE-CE for the support of the PhD student Alexandre Oliveira.

References

Aguilar, R.; Nakamatsu, J., Ramírez, E.; Elgegren, M.; Ayarza, J.; Kim, S.; Pando, M. A.; Ortega-San-Martin, L. (2016). The potential use of chitosan as a biopolymer additive for enhanced mechanical properties and water resistance of earthen construction. Construction and Building Materials 114, 625–637. http://dx.doi.org/10.1016/j.conbuildmat.2016.03.218

ASTM D2240 (2000). Standard test method for rubber property – Durometer hardness. ASTM.

Botas, S.; Veiga, M. R.; Velosa, A. (2015). Adhesion of air lime-based mortars to old tiles: moisture and open porosity influence in tile/mortar interfaces. Journal Materials in Civil Engineering, 1449-1459. https://doi.org/10.1061/(ASCE)MT.1943-5533.0001108

Cizer, Ö.; Agudo, E. R.; Navarro, C. R. (2017). Kinetic effect of carbonic anhydrase enzyme on the carbonation reaction of lime mortar. International Journal of Architectural Heritage. https://doi.org/10.1080/15583058.2017.1413604

Damas, A. L.; Veiga, M. R.; Faria, P.; Silva, A. S. (2018). Characterisation of old azulejos setting mortars: A contribution to the conservation of this type of coatings. Construction and Building Materials 171, 128-139. https://doi.org/10.1016/j.conbuildmat.2018.03.103

Delgado Rodrigues, J. (2020). Practical evidence and experimental demonstration of the Liesegangphenomenon in the carbonation process of lime mortars in exposed masonries. Journal of Cultural Heritage. https://doi.org/10.1016/j.culher.2020.02.015

Dove, C. A.; Bradley, F. F.; Patwardhan, S. V. (2016). Seaweed biopolymers as additives for unfired clay bricks. Materials and Structure 49, 4463–4482. http://dx.doi.org/10.1617/s11527-016-0801-0

EN 459-1 (2015). Building lime. Part 1: Definitions, specifications and conformity criteria. CEN, Brussels.

EN 772-21 (2011). Methods of test for masonry units. Determination of water absorption of clay and calcium silicate masonry units by cold water absorption. CEN, Brussels.

EN 998-1 (2016). Specification for mortar for masonry. Part 1: Rendering and plastering mortar. CEN, Brussels.

EN 1015-1/A1 (1998/2006). Methods of test for mortar for masonry. Part 1: Determination of particle size distribution (by sieve analysis). CEN, Brussels.

EN 1015-3 (1999). Determination of consistence of fresh mortar (by flow table). CEN, Brussels.

EN 1015-10/A1 (1999/2006). Determination of dry bulk density of hardened mortar. CEN, Brussels.

EN 1015-11 (1999). Determination of flexural and compressive strength of hardened mortar. CEN, Brussels.

EN 15801 (2009). Conservation of cultural property – Test methods – Determination of water absorption by capillarity. CEN, Brussels.

EN 16322 (2013). Conservation of cultural property – Test methods – Determination of drying properties. CEN, Brussels.

Faria, P.; Henriques, F.; Rato, V. (2008). Comparative evaluation of lime mortars for architectural conservation. Journal of Cultural Heritage 9, 338-346. https://doi.org/10.1016/j.culher.2008.03.003

Faria, P.; Martins, A. (2013). Influence of lime type and curing conditions on lime and lime-

metakaolin mortars. Durability of Building Materials and Components (V.P.de Freitas, J.M.P.Q. Delgado, eds.), Building Pathology and Rehabilitation, vol. 3, VIII, 105-126. Springer-Verlag, Berlin-Heidelberg. http://link.springer.com/chapter/10.1007/978-3-642-37475-3_5

Fang, S.; Zhang, K.; Zhang, H.; Zhang, B. (2015). A study of traditional blood lime mortar for restoration of ancient buildings. Cement and Concrete Research 76, 232-241. http://dx.doi.org/10.1016/j.cemconres.2015.06.006

Franzoni, E.; Pigino, B.; Leemann, A.; Lura, P. (2014). Use of TEOS for fired-clay bricks consolidation. Materials and Structures 47, 1175–1184. http://doi.org/10.1617/s11527-013-0120-7

Gameiro, A.; Santos-Silva, A.; Faria, P.; Grilo, J.; Branco, T.; Veiga, R.; Velosa, A. (2014). Physical and chemical assessment of air lime-metakaolin mortars: Influence of binder:aggregate ratio. Cement and Concrete Composites 45, 264-271. http://dx.doi.org/10.1016/j.cemconcomp.2013.06.010

Gandia, R.; Corrêa, A.; Gomes, F.; Marin, D.; Santana, L. (2019). Physical, mechanical and thermal behavior of adobe stabilized with "synthetic termite saliva". Engenharia Agrícola 39 (2), 139-149. http://dx.doi.org/10.1590/1809-4430

Garcia-Gonzalez, J.; Pereira, A. S.; Lemos, P. C.; Almeida, N.; Silva, V.; Candeias A.; Juan-Valdés, A.; Faria, P. (2020). Effect of surface biotreatments on construction materials. Construction and Building Materials 241. https://doi.org/10.1016/j.conbuildmat.2020.118019

Garijo, L.; Zhang, X.; Ruiz, G.; Ortega, J.J. (2020). Age effect on the mechanical properties of natural hydraulic and aerial lime mortars. Construction and Building Materials 236, 117573. https://doi.org/10.1016/j.conbuildmat.2019.117573

Gour, K. A.; Ramadoss, R.; Selvaraj, T. (2018). Revamping the traditional air lime mortar using the natural polymer – Areca nut for restoration application. Construction and Building Materials 164, 255-264. https://doi.org/10.1016/j.conbuildmat.2017.12.056

Hansen, E.; Doehne, E.; Fidler, J.; Larson, J.; Martin, B.; Matteini, M.; Rodrigues-Navarro, C.; Pardo, E. S.; Price, C.; Tagle, A.; Teutonico, J.M.; Weiss, N. (2003). A review of selected inorganic consolidants and protective treatments for porous calcareous materials. Studies in Conservation 48,

13-25. http://doi.org/10.1179/sic.2003.48.Supplement-1.13

Ivanov, V.; Chu, J.; Stabnikov, V. (2014), Iron- and calcium-based biogrouts for porous soils. Construction Materials 167, 36-41. http://dx.doi.org/10.1680/coma.12.00002

Izaguirre, A.; Lanas, J.; Álvarez, J. I. (2011). Characterization of aerial lime-based mortars modified by the addition of two different water-retaining agents. Cement and Concrete Composites 33, 309–318. https://doi.org/10.1016/j.cemconcomp.2010.09.008

Joshi, S.; Goyal, S.; Reddy, M. S. (2018). Influence of nutrient components of media on structural properties of concrete during biocementation. Construction and Building Material 158, 601–613. https://doi.org/10.1016/j.conbuildmat.2017.10.055

Keykha, H. A.; Asadi, A.; and Zareian, M. (2017). Environmental factors affecting the compressive strength of microbiologically induced calcite precipitation-treated soil. Geomicrobiology Journal 34, 889-894. https://doi.org/10.1080/01490451.2017.1291772

Lanas, J.; Alvarez, J.I. (2003). Masonry repair lime-based mortars: Factors affecting the mechanical behavior. Cement and Concrete Research 33, 1867-1876. https://doi.org/10.1016/S0008-8846(03)00210-2

Lawrence, R.M.H.; Mays, T.J.; Walker, P.; Ayala, A.A. (2006). Determination of carbonation profiles in non-hydraulic lime mortars using thermogravimetric analysis. Thermochimica Acta 444, 179–189. https://doi.org/10.1016/j.tca.2006.03.002

Liu, H.; Zhao, Y.; Peng, C.; Song, S.; Lopez-Valdivieso, A. (2016). Improvement of compressive strength of lime mortar with carboxymethyl cellulose. Journal of Materials Science 51, 9279–9286. https://doi.org/10.1007/s10853-016-0174-3

Liu, H.; Zhao, Y.; Peng, C.; Song, S.; López-Valdivieso, A. (2018). Lime mortars – The role of carboxymethyl cellulose on the crystallization of calcium carbonate. Construction and Building Materials 168, 169-177. https://doi.org/10.1016/j.conbuildmat.2018.02.119

Lors, C.; Ducasse-Lapeyrusse, J.; Gagné, R.; Damidot, D. (2017). Microbiologically induced calcium carbonate precipitation to repair microcracks remaining after autogenous healing of mortars. Construction and Building Materials 141, 461–469.

http://dx.doi.org/10.1016/j.conbuildmat.2017.03.026

Luo, J.; Chen, X.; Crump, J.; Zhou, H.; Davies, D. G.; Zhou, G.; Zhang, N.; Jin, C. (2018). Interactions of fungi with concrete: Significant importance for bio-based self-healing concrete. Construction and Building Materials 164, 275–285. https://doi.org/10.1016/j.conbuildmat.2017.12.233

Molina, W. M.; Guzmán, E. M. A.; García, H. L. C.; Arcos, J. C. A.; Acosta, A. A. T.; Arroyo, J. A. B.; Gómez, C. L.; Palomares A. A. (2014). Influence of the organic and mineral additions in the porosity of lime mortars. Advanced Materials Research 887, 830–837. https://doi.org/10.4028/www.scientific.net/AMR.887-888.830

Naeimi, M.; Chu, J.; Haddad, A. (2016). Comparison of chemical source and microbially produced ferrous cations for iron-based biocementation of sand. Iranian Journal Science and Technolology 40, 149-157. https://doi.org/10.1007/s40996-016-0015-2

Nakamatsu, J.; Kim, S.; Ayarza, J.; Ramírez, E.; Elgegren, M.; Aguilar, R. (2017). Eco-friendly modification of earthen construction with carrageenan: Water durability and mechanical assessment. Construction and Building Materials 139, 193–202. http://dx.doi.org/10.1016/j.conbuildmat.2017.02.062

Nardi, C.; Cecchi, A.; Ferrara, L.; Benedetti, A.; Cristofori, D. (2017). Effect of age and level of damage on the autogenous healing of lime mortars. Composites Part B: Engineering 124, 144-157. https://doi.org/10.1016/j.compositesb.2017.05.041

Nunes, C.; Slížková, Z. (2014). Hydrophobic lime-based mortars with linseed oil: Characterization and durability assessment. Cement and Concrete Research 61, 28-39. http://dx.doi.org/10.1016/j.cemconres.2014.03.011

Nunes, C.; Viani, A.; Ševcík, R. (2020). Microstructural analysis of lime paste with the addition of linseed oil, stand oil, and rapeseed oil. Construction and Building Materials 238, 117780. https://doi.org/10.1016/j.conbuildmat.2019.117780

Oliveira, A.; Faria, P.; P.C. Lemos; Guerra, J.; Candeias, A.; Pereira, A.S. (submitted). Biotreatment of ceramic bricks: the impact of the application method of an innovative bioproduct on

biomineralization.

Omoregie, A. I.; Khoshdelnezamiha, G.; Senian, N.; Ong. D. E. L., Nissom, P. M. (2017). Experimental optimisation of various cultural conditions on urease activity for isolated sporosarcina pasteurii strains and evaluation of their biocement potentials. Ecological Engineering 109, 65-75. https://doi.org/10.1016/j.ecoleng.2017.09.012

Pahlavan, P.; Manzi, S.; Sansonetti, A.; Bignozzi, M. C. (2018). Valorization of organic additions in restorative lime mortars: Spent cooking oil and albumen. Construction and Building Materials 181, 650–658. https://doi.org/10.1016/j.conbuildmat.2018.06.089

Parracha, J. L.; Pereira, A. S.; da Silva, R. V.; Almeida, N.; Faria, P. (2019). Efficacy of iron-based bioproducts as surface biotreatment for earth-based plastering mortars. Journal of Cleaner Production 237, 117803. https://doi.org/10.1016/j.jclepro.2019.117803

RILEM II 8b (1980). Water drop absorption: recommended tests to measure the deterioration of stone and to assess the effectiveness of treatment methods. Materials and Structutures 13, 175-253. https://doi.org/10.1007/BF02473564

Rossi-Doria, P.R. (1986). Mortars for restoration: basic requirements and quality control. Materials and Structures 19, 199-203. https://doi.org/10.1007/BF02472148

Schaumann, G. E.; Braun, B.; Kirchner, D.; Rotard, W.; Szewzyk, U.; Grohmann E. (2007). Influence of biofilms on the water repellency of urban soil samples. Hydrological Processes 21, 2276-2284. https://doi.org/10.1002/hyp.6746

Schwantes-Cezario, N.; Camargo, G. S.; Couto, A. F.; Porto, M. F.; Cremasco, L. V, Andrello, A. C.; Toralles, B. M. (2020). Mortars with the addition of bacterial spores: Evaluation of porosity using different test methods. Journal of Building Engineering 30, 101235. https://doi.org/10.1016/j.jobe.2020.101235

Seifan, M.; Sarmah, A. K.; Ebrahiminezhad, A.; Ghasemi, Y.; Samani, A. K.; Berenjian, A. (2018). Bio-reinforced self-healing concrete using magnetic iron oxide nanoparticles. Applied Microbiology and Biotechnology 102, 2167–2178. https://doi.org/10.1007/s00253-018-8782-2

Silva, B. A.; Pinto, A. P. F.; Gomes, A. (2015). Natural hydraulic lime versus cement for blended

lime mortars for restoration works. Construction and Building Materials 94, 346–360. http://dx.doi.org/10.1016/j.conbuildmat.2015.06.058

Silva, B.A.; Pinto A.P.F.; Gomes, A.; Candeias, A. (2020). Impact of a viscosity-modifying admixture on the properties of lime mortars. Journal of Building Engineering 31, 101132. https://doi.org/10.1016/j.jobe.2019.101132

Son, H. M.; Kim, H. Y.; Park, S. M.; Lee, H. K. (2018). Ureolytic/non-ureolytic bacteria co-cultured self-healing agent for cementitious materials crack repair. Materials 11. https://doi.org/10.3390/ma11050782

Stabnikov, V.; Ivanov, V. (2016). Biotechnological production of biogrout from iron ore and cellulose. Journal of Chemical Technology and Biotechnology 92, 180-187. https://doi.org/10.1002/jctb.4989

Van Hees, R. P. J.; Binda, L.; Papayianni, I.; Toumbakari, E. (2004). Characterisation and damage analysis of old mortars. Materials and Structures 37, 644-648. https://doi.org/10.1007/BF02483293

Vashisht, R.; Attri, S.; Sharma, D.; Shukla, A.; Goel, G. (2018). Monitoring biocalcification potential of *Lysinibacillus sphaericus* isolated from alluvial soils for improved compressive strength of concrete. Microbiological Research 207, 226–231. https://doi.org/10.1016/j.micres.2017.12.010

Veiga, R. (2017). Air lime mortars: What else do we need to know to apply them in conservation and rehabilitation interventions? A review. Construction and Building Materials 157, 132–140. https://doi.org/10.1016/j.conbuildmat.2017.09.080

Veiga, M. R.; Fragata, A.; Velosa, A. L.; Magalhães, A. C.; Margalha, G. (2010). Lime-based mortars: viability for use as substitution renders in historical buildings. International Journal of Architectural Heritage 4, 177–195. https://doi.org/10.1080/15583050902914678

Ventolà, L.; Vendrell, M.; Giraldez, P.; Merino, L. (2011). Traditional organic additives improve lime mortars: New old materials for restoration and building natural stone fabrics. Construction and Building Materials 25, 3313–3318. https://doi:10.1016/j.conbuildmat.2011.03.020

Wang, X. F.; Zhang, J. F.; Zhao, W.; Han, R.; Han, N. X.; Xing, F. (2018). Permeability and pore structure of microcapsule-based self-healing cementitious composite. Construction and Building

Materials 165, 149-162. https://doi.org/10.1016/j.conbuildmat.2017.12.008

Zhang, J.; Liu, Y.; Feng, T.; Zhou, M.; Zhao, L.; Zhau, A.; Li, Z. (2017). Immobilizing bacteria in expanded perlite for the crack self-healing in concrete. Construction and Building Materials 148, 610–617. http://dx.doi.org/10.1016/j.conbuildmat.2017.05.021